PHYSICAL REVIEW B **76**, 161308(R) (2007)

Spin-state mixing in InAs double quantum dots

A. Pfund, I. Shorubalko, K. Ensslin, and R. Leturcq*
Solid State Physics Laboratory, ETH Zürich, 8093 Zürich, Switzerland
(Received 10 September 2007; published 12 October 2007)

We quantify the contributions of hyperfine and spin-orbit-mediated singlet-triplet mixing in weakly coupled InAs quantum dots by electron transport spectroscopy in the Pauli spin-blockade regime. In contrast to double dots in GaAs, the spin-orbit coupling is found to be more than two orders of magnitudes larger than the hyperfine mixing energy. It is already effective at magnetic fields of a few mT, where deviations from pure hyperfine mixing are observed.

DOI: 10.1103/PhysRevB.76.161308 PACS number(s): 73.63.Kv, 72.25.−b

Spin dependent interactions such as spin-orbit (SO) interactions and hyperfine (HF) coupling to nuclei have a significant influence on the spin transport in solid-state devices. The perspective of active control of these mechanisms stimulated many proposals for "spintronic" devices.[1,2] Spin states in coupled semiconductor quantum dots are considered as possible realizations of quantum bits in scalable solid-state quantum computers.[3] Electrical control of SO interactions[4,5] as well as dynamic coupling of electrons and nuclei[6,7] could provide a convenient way for qubit operations. However, both effects are at the same time a major source of perturbation, since spin-state mixing enables various paths of spin relaxation.[8–11] In GaAs double quantum dots (DQDs), HF interactions have been identified to dominate the spin mixing at small magnetic fields, while SO interactions are not relevant in this regime.[12–15] In single quantum dots, SO is the main source for spin relaxation, especially at high magnetic fields.[9,11,16,17]

These properties are specific for every particular material. Spin-orbit interactions and the coupling to magnetic fields are expected to be orders of magnitudes stronger in InAs compared to GaAs. The interplay of relaxation processes mediated by SO and HF interactions[18] can lead to an effectively suppressed spin relaxation, which requires strongly coupled dots. In order to quantify the relevant energy scales, we study the leakage current in the Pauli spin-blockade regime for a weakly coupled DQD. In contrast to strongly coupled dots, inelastic relaxation currents are weak and transport occurs for aligned levels due to the mixing of spin states.

More precisely, we investigate mixing of singlet (S) and triplet (T) states in a weakly coupled InAs DQD. Transport spectroscopy in the Pauli spin-blockade regime allows one to identify the relevant spin states. We are able to distinguish the contributions of HF and SO coupling for small and large magnetic fields. Similar to recent experiments in single InAs dots,[19] we observe a strong SO-induced S-T mixing at large magnetic fields corresponding to a coupling energy of $\Delta_{SO}=0.2$ meV. The mixing energy by the uncorrelated hyperfine fields in the two dots is found to be close to three orders of magnitude smaller for small external fields. In contrast to GaAs DQDs, we observe clear deviations from the previously studied[12,14] HF mixing already at millitesla fields, which can be attributed to SO interactions.

The device is fabricated in an InAs nanowire, catalytically grown by metal organic vapor phase epitaxy. The wire diameter is around 100 nm. Three top gates of 70 nm width and separation define a serial DQD along the nanowire[20] (NW) [Fig. 1(a)]. We refer to the two outer gates as $G1$ and $G2$ (tuning energy levels in dots 1 and 2) and to the center gate as GC (tuning the interdot coupling). Transport measurements were performed in a dilution refrigerator at an electronic temperature of ~100 mK and with a magnetic field aligned perpendicular to the nanowire axis.

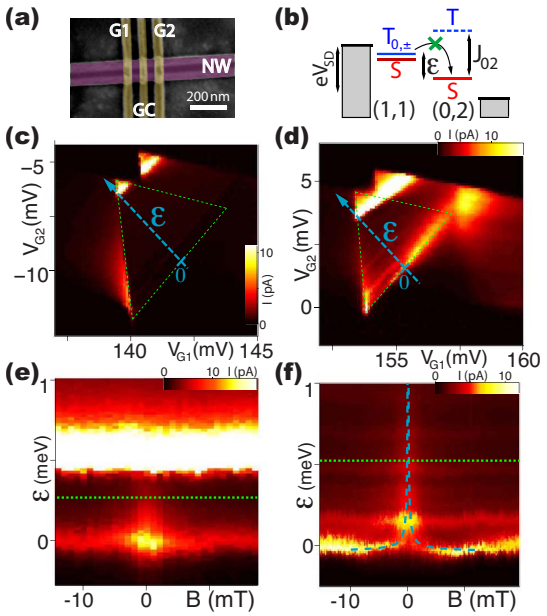

FIG. 1. (Color online) (a) Scanning electron image of a representative device. Cr/Au top gates $G1$ and $G2$ and GC define a double quantum dot in the InAs nanowire (NW). (b) Energy diagram for sequential transport through a two-electron double dot at finite bias V_{SD}. For small detuning ε between (1,1) and (0,2) ground states, Pauli spin blockade suppresses transport once the second electron enters in a (1,1) triplet. For $\varepsilon > J_{02}$, transport via triplet states is allowed. (c) Double-dot current I_{SD} for $V_{SD}=2$ mV as a function of gate voltages V_{G1} and V_{G2}. The coupling gate voltage is fixed at $V_{GC}=-120$ mV. Spin blockade suppresses current in the base region of the triangle. Along the dashed line, the dot levels are detuned by an energy ε. (d) Same for weaker coupling $V_{GC}=-170$ mV ($V_{SD}=1.6$ mV). (e) Plot of I_{SD} in dependence of detuning ε and magnetic field B for $V_{GC}=-180$ mV. (f) Same for $V_{GC}=-170$ mV. Dashed lines are fits to a model for tunnel-coupled levels ($t=6$ μeV, $|g^*|=7$); see text.

We could tune the three gates to create two weakly coupled quantum dots. The states can then be labeled by the occupation numbers (n,m) for dots 1 and 2. For finite bias voltage V_{SD}, electron transport is forbidden due to Coulomb blockade everywhere except for triangular regions in the $V_{G1}-V_{G2}$ plane[21] [dashed lines in Figs. 1(c) and 1(d)]. Here, the dot states are in the bias window and sequential transport through the serial dots is possible. In Fig. 1(c), a measurement of the current I_{SD} through the DQD is shown for $V_{SD}=2$ mV. Transport is strongly suppressed in the base region of the triangle, but not at the corner points and side edges. This can be explained by Pauli spin blockade (SB).[22] Considering the DQD in an initial (0,1) state, a second electron can be loaded into either the singlet $S(1,1)$ or a (1,1) triplet [named $T_m(1,1)$ with $m=0,\pm1$ according to the z component of the spin]. The ground state of the (0,2) configuration at zero B field is a singlet. Sequential transport is therefore blocked due to spin conservation, once the second electron entered the DQD in a (1,1) triplet [Fig. 1(b)]. This SB is lifted if the detuning ε between the (1,1) and (0,2) states exceeds the (0,2) singlet-triplet splitting J_{02}, which gives rise to a strong current in the tip of the triangle [Fig. 1(c)]. We estimate a total number of $\sim$10 electrons in the DQD. In the following, the labels for the spin states therefore refer to the number of excess electrons assuming a spinless inert core of electrons (for similar arguments in a GaAs DQD see Ref. 23).

In Fig. 1(d), the same triangle is shown for weaker interdot coupling. Similar to experiments in GaAs,[12] leakage current occurs around $\varepsilon=0$, while SB is preserved at larger detuning. A large current is again observed for $\varepsilon>J_{02}$ at the tip of the triangle. Compared to Fig. 1(c), the splitting J_{02} is decreased due to the change of confinement.[24]

In order to identify the spin states responsible for the leakage current, we study I_{SD} as a function of magnetic field and level detuning ε. While ε changes the energy separation between (1,1) and (0,2) states, B mainly induces a Zeeman splitting between the spin-polarized triplets $T_{\pm}$ and the unpolarized T_0 and S. To evaluate ε, gate voltages have been transformed into energy using the lever arms obtained by relating the size of the triangles to the bias voltage.[21] Figures 1(e) and 1(f) show measurements for two different center gate settings, but both still corresponding to weak coupling. Similar to Ref. 12, the current for finite ε is reduced already at fields of a few mT. In the case of slightly stronger coupling [Fig. 1(f)], the peak splits into characteristic wings around $B=0$ that merge at higher detuning ε.

The base line corresponding to $\varepsilon=0$ at small B cannot be suppressed completely even for large fields. The continuation of Fig. 1(f) up to $B=5$ T is shown in Fig. 2. The base line shifts linearly between 0 T and 2 T. The top peak corresponding to transport through (0,2) triplets is separated by $J_{02}=1.1$ meV at $B=0$. It splits into three branches with very different current levels (dashed lines). At $B\approx2.7$ T, a pronounced anticrossing of the two lowest peaks occurs.

To understand the origin of the leakage current in the low-field regime, we plot the detuning dependence of the relevant DQD levels around $\varepsilon\approx0$ in Fig. 3(c), as obtained in a Hund-Mulliken model.[25] A tunnel coupling t hybridizes the singlets $S(1,1)$ and $S(0,2)$. This is visible as an anticrossing

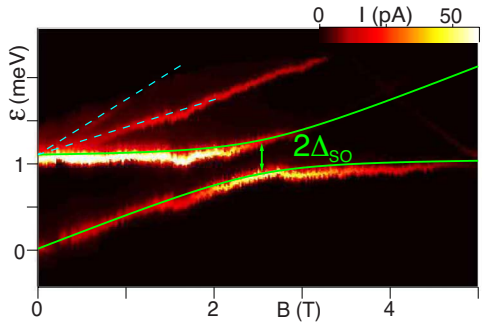

FIG. 2. (Color online) Current as a function of detuning ε and magnetic field B as in Fig. 1(f), but on a larger field scale. The lines show fits to the model described in the text ($\Delta_{SO}=200$ μeV, $|g^*|=7$, $|g_2^*|=5.5$). An overal shift of 0.3 meV/T has been removed, which could be due to orbital effects.

of $\sim 2t$ between the branches S. An external field B splits the triplets by a Zeeman energy $g^*\mu_B B$, where g^* is the effective g factor and μ_B is the Bohr magneton.

Enhanced current around $B\approx0$ and $\varepsilon\approx0$ could be explained with HF mixing.[12,14] The HF coupling can be expressed by a random nuclear field as a cumulative effect of those nuclei that overlap with the electronic wave function.[26] The distribution of this effective field is characterized by the width B_N, which is a measure for the amplitude of the field fluctuations.[26] This mixing is efficient for the (1,1) singlets and triplets where electrons are distributed over different dots.

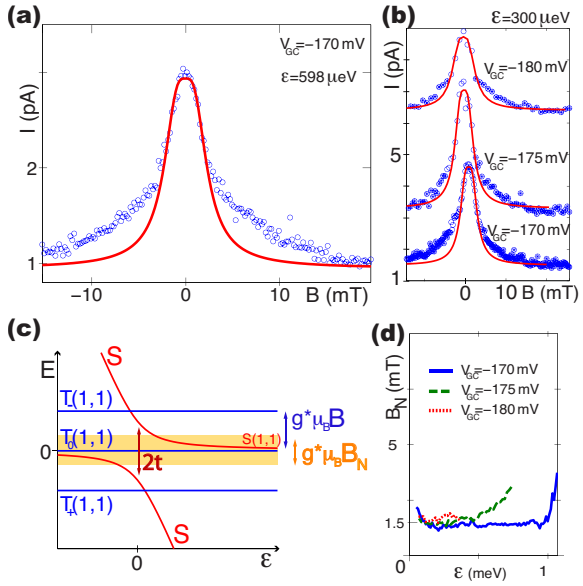

FIG. 3. (Color online) (a) Circles: cut along the dotted green line in Fig. 1(f). The solid red line is a fit of the center peak with Eq. (11) of Ref. 14. (b) Similar traces along the dotted line in Fig. 1(e) for three different values of the coupling gate V_{GC}. Solid red lines are fits of the center peaks. (c) Level scheme of the singlets S and the (1,1) triplets around zero detuning ε. The tunnel coupling t induces an anticrossing of the hybridized singlets. The Zeeman energy $g^*\mu_B B$ splits the triplets. A random nuclear field with amplitude B_N mixes the states in the shaded region. (d) Extracted B_N from the central peak fits as a function of detuning for different couplings.

A (1,1) triplet is mixed to $S(1,1)$ if their splitting Δ_{ST} is smaller than the HF coupling, quantified by $g^*\mu_B B_N$. This regime is indicated by the shaded region around $B=0$ in Fig. 3(c). An external field B splits the triplets $T_\pm(1,1)$ from $S(1,1)$, and SB is recovered by these states. In the limit $g^*\mu_B B_N > \Delta_{ST}$, this leads to a current peak around $B=0$. For very weak coupling as in Fig. 1(e), the anticrossing of the S branches is narrow and the above condition is always fulfilled. For stronger coupling [Fig. 1(f)], it can be achieved at finite detuning, as obvious from Fig. 3(c). A quantitative description for the B dependence of the current was obtained assuming a classical distribution of stationary random nuclear fields.[14] This has been used to quantify the HF coupling in GaAs DQDs.[12]

In Fig. 3(a) we plot a current trace (circles) as a a function of B for fixed detuning, indicated by the dotted line in Fig. 1(f). The complete data cannot be fitted satisfactory with a single curve according to Eq. (11) of Ref. 14. This feature is consistently observed for different values of interdot coupling, as shown in Fig. 3(b). Nevertheless, a fit to the central peak leaving out the wide tails for $|B|>3$ mT leads to good agreement. From these fits, we extract $B_N \approx 1.5 \pm 0.2$ mT for the effective field amplitude. This result is almost independent of interdot coupling and detuning as shown in Fig. 3(d), supporting the validity of the model in Ref. 14 [the increase for large ε can be explained by the proximity of the (0,2) triplets]. The value corresponds to the HF fluctuation amplitude of $N \approx 0.5 \times 10^5$ nuclei,[27] which is consistent with the dot size evaluated from charging energy and excited state spectrum.[20]

For increased tunnel coupling t, the anticrossing is larger and $T_{0,\pm}(1,1)$ are separated from S for small B and ε. Increasing B, the triplet $T_-(1,1)$ is again mixed to the upper singlet branch, which has (1,1) character for small detuning. This explains the splitting of the current peak around $B=0$ into wings, as observed in Fig. 1(f). Fitting the upper singlet branch [see Fig. 3(c)] in the vicinity of the anticrossing to the wings in Fig. 1(f) allows one to quantify the tunnel coupling $t=6$ μeV (using $|g^*|=7$ as determined below).

The deviation of the leakage current for finite fields ($|B|>3$ mT) is the most surprising result of our work and has not been observed in GaAs DQDs.[12] Before discussing the possible origin, we note that in the model of Ref. 14, additional spin-mixing mechanisms are neglected. This is justified by the experimental results on DQDs fabricated in GaAs.[12]

In the case of InAs, other sources of mixing such as SO interactions could play a role even at small magnetic fields. The importance of SO interactions in our InAs DQDs is confirmed by the measurement shown in Fig. 2. To interpret the observed current peaks and their magnetic field dependence, we extend the scheme for the detuning dependence of the DQD states as shown in Fig. 4. At $B=0$, the (0,2) triplets are separated from $S(0,2)$ by J_{02}. A tunnel coupling t that hybridizes states with equal spin quantum numbers leads to anticrossings. For weakly coupled dots, sequential tunneling is the strongest transport path and resonant current peaks occur at those detunings ε, where (1,1) and (0,2) states are mixed by one of the described mechanisms.

The strongest current line occurs at a detuning corresponding to $J_{02}=1.1$ meV at $B=0$. We relate this peak to tunnel mixing of (1,1) and (0,2) triplets with the *same* spin quantum number $m=0,\pm 1$. The corresponding anticrossings are labeled X in Fig. 4. If the effective g factors g^* for $T_\pm(1,1)$ and g_2^* for $T_\pm(0,2)$ are close, all three anticrossings occur at almost the same B-independent detuning and give rise to a single peak.

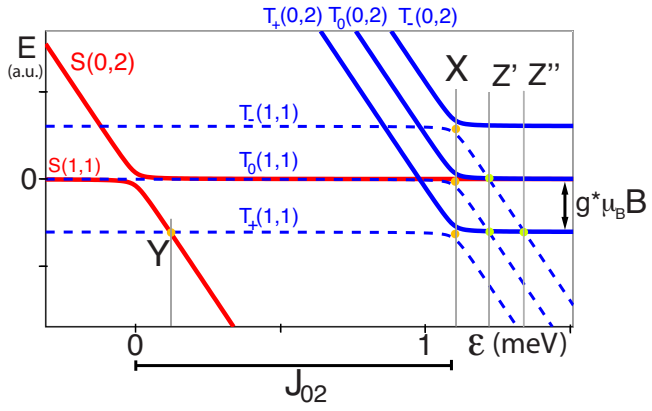

FIG. 4. (Color online) Energies of the relevant states in the spin-blockade regime as a function of detuning ε. J_{02} denotes the (0,2) singlet-triplet splitting. A tunnel coupling energy t mixes states with the same spin quantum numbers, leading to anticrossings around $\varepsilon \approx 0$, and at the points marked with X. In the figure, a magnetic field B with $g^*\mu_B B \gg t$ splits the triplets. Spin-flip processes can also lead to mixing at other degeneracy points such as Y and Z', Z''.

The lowest line in Fig. 2 shifts linearly in B up to ~ 2 T. We explain it by probing the lower singlet branch with the state $T_+(1,1)$, which is split from $T_0(1,1)$ by $g^*\mu_B B$ (see Fig. 4). At the degeneracy point of both states (labeled Y), HF and SO mix S and T_+. The resonant current involves a first-order spin flip[28] and is consequently weaker than the tunnel peak X. From the slope, we extract an effective g factor $|g^*|=7$ for the (1,1) triplets. We note that we did not compensate for a quadratic shift in B, which would be the expected orbital effect of the magnetic field in single dots.[29]

The two upper lines in Fig. 2 are much weaker than the peak due to tunnel coupling. Comparing to Fig. 4, we suggest that these lines arise from the degeneracies named Z' and Z''. The involved mixing processes require higher-order spin flips. This is consistent with the much weaker intensity of these current peaks. This model is also supported by the g factor $|g_2^*|=5.5$ extracted from the slopes of the upper lines. In contrast to (1,1) triplets, the relevant states $T_\pm(0,2)$ involve excited orbital states of dot 2, which could explain the difference between g^* and g_2^*.[19] To further test the consistency, we opened $G1$ and studied the B-field dependence of the excited states in the single dot 2 with the same electronic occupation. This yielded again $|g_2^*|=5.5$ (not shown).

If $g^*\mu_B B$ approaches J_{02}, the singlet $S(0,2)$ becomes degenerate with $T_+(0,2)$. We observe a pronounced anticrossing of the lower two lines with $2\Delta_{SO} \approx 0.4$ meV. Similar to recent measurements in InAs single dots,[19] this can be explained by SO interactions. Contributions of the HF interaction are expected to be negligible in this situation, since electrons in (0,2) states experience the same nuclear field.[9,15,17]

Using $|g^*|=7$ and $J_{02}=1.1$ meV we can overlay energies from a simple model of two-level repulsion to the current peaks in Fig. 2 (green lines) with reasonable agreement and obtain a coupling matrix element $\langle S(0,2)|H_{SO}|T_+(0,2)\rangle = \Delta_{SO}=0.2$ meV.

We now return to the discussion of the wide current peaks [Figs. 3(a) and 3(b)], which are not reproduced by the model in Ref. 14. Since we observed a much stronger SO interaction than in GaAs, we suggest that the wide tails of the current peaks are related to this additional mixing. Singlets and $(m=\pm 1)$ triplets are also hybridized by the SO coupling. This enhances the anticrossing of those levels. The resulting states therefore sustain a singlet contribution up to larger Zeeman splitting, and hence a higher external field is required to recover spin blockade by the $T_{\pm}(1,1)$ states. We note that the field scale of the wide tails ($\sim$10 mT) agrees with the onset of inelastic spin relaxation for strongly coupled InAs dots in Ref. 18, which was related to the influence of SO interaction.

Beyond that, taking into account the coherent dynamics of the coupled nuclear and electron spins[30] may significantly change the predictions of Ref. 14.

In conclusion we measured the HF and SO mixing energies of singlets and triplets in a weakly coupled InAs DQD in the regime of Pauli spin blockade. We were able to extract all relevant energy scales of the DQD and find a hierarchy $J_{02} \gtrsim \Delta_{SO} \gg t \gtrsim g^* \mu_B B_N$. In contrast to DQDs in GaAs, SO interactions are efficient for small fields of a few mT. These energy scales suggest that InAs DQDs are suitable candidates for electric-field-induced spin manipulation.[4,5]

We thank T. Ihn, D. Loss, and J. Taylor for stimulating discussions and M. Borgström and E. Gini for advice on nanowire growth. We acknowledge financial support from the ETH Zurich, and I.S. thanks the European Commission for a grant.

*leturcq@phys.ethz.ch

[1] S. A. Wolf *et al.*, Science **294**, 1488 (2001).
[2] S. Datta and B. Das, Appl. Phys. Lett. **56**, 665 (1990).
[3] D. Loss and D. P. DiVincenzo, Phys. Rev. A **57**, 120 (1998).
[4] V. N. Golovach, M. Borhani, and D. Loss, Phys. Rev. B **74**, 165319 (2006); D. V. Bulaev and D. Loss, Phys. Rev. Lett. **98**, 097202 (2007).
[5] C. Flindt, A. S. Sørensen, and K. Flensberg, Phys. Rev. Lett. **97**, 240501 (2006).
[6] B. E. Kane, Nature (London) **393**, 133 (1998).
[7] K. Ono and S. Tarucha, Phys. Rev. Lett. **92**, 256803 (2004).
[8] S. I. Erlingsson, Y. V. Nazarov, and V. I. Falko, Phys. Rev. B **64**, 195306 (2001).
[9] V. N. Golovach, A. Khaetskii, and D. Loss, Phys. Rev. Lett. **93**, 016601 (2004).
[10] S. Sasaki, T. Fujisawa, T. Hayashi, and Y. Hirayama, Phys. Rev. Lett. **95**, 056803 (2005).
[11] T. Meunier, I. T. Vink, L. H. Willems van Beveren, K. J. Tielrooij, R. Hanson, F. H. Koppens, L. Tranitz, W. Wegscheider, L. P. Kouwenhoven, and L. M. K. Vandersypen, Phys. Rev. Lett. **98**, 126601 (2007).
[12] F. H. L. Koppens *et al.*, Science **309**, 1346 (2005).
[13] A. C. Johnson *et al.*, Nature (London) **435**, 925 (2005).
[14] O. N. Jouravlev and Y. V. Nazarov, Phys. Rev. Lett. **96**, 176804 (2006).
[15] A. V. Khaetskii, D. Loss, and L. Glazman, Phys. Rev. Lett. **88**, 186802 (2002).
[16] S. Amasha *et al.*, arXiv:cond-mat/0607110 (unpublished).
[17] A. V. Khaetskii and Y. V. Nazarov, Phys. Rev. B **64**, 125316 (2001).
[18] A. Pfund, I. Shorubalko, K. Ensslin, and R. Leturcq Phys. Rev. Lett. **99**, 036801 (2007).
[19] C. Fasth, A. Fuhrer, L. Samuelson, V. N. Golovach, and D. Loss, Phys. Rev. Lett. **98**, 266801 (2007).
[20] A. Pfund, I. Shorubalko, R. Leturcq, and K. Ensslin, Appl. Phys. Lett. **89**, 252106 (2006).
[21] W. G. van der Wiel *et al.*, Rev. Mod. Phys. **75**, 1 (2003).
[22] K. Ono, D. G. Austing, Y. Tokura, and S. Tarucha, Science **297**, 1313 (2002).
[23] H. W. Liu, T. Fujisawa, T. Hayashi, and Y. Hirayama, Phys. Rev. B **72**, 161305(R) (2005).
[24] L. P. Kouwenhoven, D. G. Austing, and S. Tarucha, Rep. Prog. Phys. **64**, 701 (2001).
[25] G. Burkard, D. Loss, and D. P. DiVincenzo, Phys. Rev. B **59**, 2070 (1999).
[26] I. A. Merkulov, A. L. Efros, and M. Rosen, Phys. Rev. B **65**, 205309 (2002).
[27] For the calculation in InAs we use the values given in J. R. Goldman, Ph.D. thesis, Stanford University, 2005.
[28] S. Dickmann and P. Hawrylak, JETP Lett. **77**, 30 (2003).
[29] S. Tarucha, D. G. Austing, T. Honda, R. J. van der Hage, and L. P. Kouwenhoven, Phys. Rev. Lett. **77**, 3613 (1996).
[30] W. A. Coish and D. Loss, Phys. Rev. B **70**, 195340 (2004).